Journal of Organometallic Chemistry 888 (2019) 16–23

Contents lists available at ScienceDirect

Journal of Organometallic Chemistry

journal homepage: www.elsevier.com/locate/jorganchem

Ferrocene appended naphthalimide derivatives: Synthesis, DNA binding, and in vitro cytotoxic activity

Deng-Guo Jia [a, 1], Jia-An Zheng [a, 1], Yan-Ru Fan [a, *], Jian-Qiang Yu [a], Xiu-Li Wu [a], Bo-Jin Wang [a], Xin-Bin Yang [b], Yu Huang [a, **]

[a] Key Laboratory of Hui Ethnic Medicine Modernization, Ministry of Education, Ningxia Engineering and Technology Research Centre of Hui Medicine Modernization, College of Pharmacy, Ningxia Medical University, 750004, Yinchuan, PR China
[b] Rongchang Campus, Southwest University, 402460, Chongqing, PR China

ARTICLE INFO

Article history:
Received 27 December 2018
Received in revised form
26 February 2019
Accepted 1 March 2019
Available online 6 March 2019

Keywords:
Naphthalimide derivatives
Ferrocene
Synthesis
Cytotoxicity
DNA binding

ABSTRACT

Three novel ferrocene appended naphthalimide derivatives (**2a**, **2b** and **6**) were synthesized and characterized by IR, ^{1}H NMR and mass spectroscopies. In electrochemical experiments, all of the ferrocene appended naphthalimide derivatives exhibited reversible one-electron oxidation in CV curves. And the DNA binding ability of the compounds was studied by ethidium bromide displacement experiments and UV−visible spectrophotometry. The ferrocene appended naphthalimide derivative **6** also exhibited the highest DNA binding ability in all the tested compounds. According to the viscosity results, all of the synthesized compounds displayed the partial intercalation binding mode to DNA duplex. Bis-naphthalimide compound **5** was used as reference compound to evaluate the synergistic effect of the ferrocene group in ferrocene appended naphthalimide derivative **6**. The cytotoxicity of the synthesized compounds against **4** different human cancer cell lines (EC109, BGC823, SGC 7901 and HepG2) was studied by MTT assay. The ferrocene appended bis-naphthalimide derivative 6 showed the best cytotoxicity against tested human cancer cells in all the synthesized naphthalimide derivatives and control drug amonafide. The uptake of naphthalimide derivative **6** was proved by laser confocal images. In addition, the DNA damage induced by naphthalimide derivative **6** was studied by comet assay.

1. Introduction

Cancer is the second cause of death and responsible for one-sixth of the deaths (estimated 9.6 million) all over the world in 2018 [1]. And the International Agency for Research on Cancer (IARC) estimated that there would be 21.7 million new cancer cases and 13 million cancer deaths by 2030 [2]. The development of new cancer treatments and drugs have been attracted great attention for decades. In 2017, FDA approved 12 oncology products which were 26% of the approved products [3].

Organometallic compounds exhibited remarkable potential for the development of new cancer drugs not only due to the direct cytotoxicity but also to the drug targeting and active anticancer immune response ability [4]. Among the organometallic compounds, ferrocene is one of the most well-known compounds in many areas of science, especially in medicinal chemistry. It attracted great attention on account of the high stability, lipophilicity, low toxicity, easy functionalization and mild reversible redox property [5]. Hence, ferrocenyl group conjugated nature products or drugs were synthesized and exhibited kinds of biological activities, including antitumor, antimalarial and antibacterial activity [6]. In the development of ferrocene based drugs, the two most successful examples were ferrocifen and ferroquine. The last one entered the clinical trials and would be completed in 2019 [7]. The two compounds represent one type of ferrocene derivatives, in which the ferrocenyl group replaced a portion of the lead compound [8]. And in another type, the ferrocenyl group directly attached to the lead compound, which is a promising strategy to enhance the anticancer efficiency by attaching ferrocenyl group to a DNA intercalator [5a]. Ferrocene appended intercalators were reported to exhibit far more cytotoxicity or better selectivity towards cancerous cells than the single intercalators [9].

* Corresponding author.
** Corresponding author.
E-mail addresses: risefyr@163.com (Y.-R. Fan), huangyunxmu@163.com (Y. Huang).
[1] The two authors contributed equally to this paper.

https://doi.org/10.1016/j.jorganchem.2019.03.001
0022-328X/

1,8-naphthalimide, a well-known DNA intercalator, has been extensively investigated in the development of antitumor agents [10]. Some of the naphthalimide derivatives, such as amonafide, elinafide and bisnafide (Fig. 1), have entered into phase II clinical trials stage [10b,11]. Among them, elinafide and bisnafide were typical bis-intercalator which constructed by a polyamine linker and two naphthalimide groups. Such a strategy was helpful to enhance the DNA binding ability and anticancer activity of the intercalator [12]. In our previous work, some bis-aryl compounds were designed and synthesized according to the strategy [13]. And the DNA binding and cytotoxicity activity of the bis-aryl compounds were systematically studied, which displayed significant advantage over the mono-aryl ones.

Herein, ferrocene appended mono-naphthalimide and bis-naphthalimide derivatives were synthesized to study the influence of linker and synergistic effect of the ferrocenyl group to naphthalimide derivatives. The cytotoxicity of the synthesized compounds against human cancer cells was evaluated by MTT assay. And the DNA binding ability of the compounds was studied by ethidium bromide (EB) displacement experiments, UV−visible spectrophotometry and viscosity studies. According to the results of experiments, suitable linker and the presence of the ferrocenyl group were helpful to enhance the cytotoxicity and the DNA binding ability of the bis-naphthalimide derivative.

2. Materials and methods

2.1. General

All of the chemical reagents and solvents were obtained from commercial sources and used directly without further purification, except THF. CT DNA was from Sigma-Aldrich. *N*-Boc-bromoethylamine was synthesized according to the literature [14]. Electrochemical experiments were performed on a CH Instruments CHI-600 electrochemical workstation. Fluorescence spectra were recorded on a Hitachi F4600 spectrofluorometer at room temperature. UV−visible data were carried out on a Shimadzu UV-2600 spectrophotometer at room temperature. IR spectra were recorded on a Shimadzu IRAffinity-1 spectrophotometer. ^{1}H NMR and ^{13}C NMR spectra were recorded on a Bruker AVIII 400 spectrometer, with tetramethylsilane (TMS) as an internal standard. Mass spectra were recorded on a Shimadzu LCMS-IT-TOF. Confocal microscopy images were captured on an Olympus FV1000-IX81 Confocal Microscope. Comet assay data were recorded with an Olympus BX53 fluorescence microscopy.

2.2. Synthesis

2.2.1. Synthesis of mono-naphthalimide derivative **1**

1,8-Naphthalimide (2 g, 10.14 mmol), hydroxyethyl amine and triphenylphosphine (5.3 g, 20.27 mmol) were dissolved in 50 mL anhydrous THF. After cooled to 0 °C in an ice-water bath, diisopropyl azodiformate (4.0 mL, 20.27 mmol) was added dropwise with stirring in 30 min. Then the mixture was stirred under the protection of nitrogen at room temperature for 5 h. After removed the solvent by rotary evaporator, the crude oil product was purified by column chromatography (ethyl acetate: methanol) to yield the pure product as a white solid.

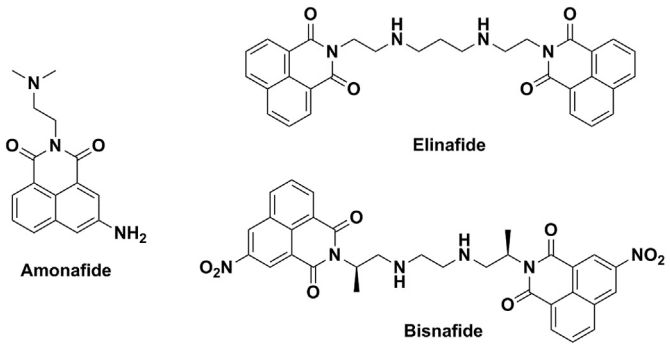

Fig. 1. Representative naphthalimide derivatives in clinical trial.

2.2.1.1. Naphthalimidoethylamine ***1a***. Yield: 51.64%. FTIR (KBr) ν: 3348(NH_2), 1698(C═O). ^{1}H NMR (400 MHz, $CDCl_3$) δ: 8.61 (dd, J = 7.2, 1.1 Hz, 2H, −ArH), 8.22 (dd, J = 8.2, 1.1 Hz, 2H, −ArH), 7.76 (dd, J = 8.2, 7.3 Hz, 2H, −ArH), 4.29 (t, J = 6.6 Hz, 2H, $-CH_2$), 3.08 (t, J = 6.6 Hz, 2H, $-CH_2$). ^{13}C NMR (100 MHz, $CDCl_3$) δ: 164.62, 134.14, 131.72, 131.46, 128.35,127.07, 122.71, 43.24, 40.64. HR-MS, m/z: $[M+H]^+$ 241.0939 (calcd for $C_{14}H_{12}N_2O_2^+$: 241.0899).

2.2.1.2. 2-(Naphthalimidoethylamino)ethylamine ***1b***. Yield: 58.33%. FTIR (KBr) ν: 3433(NH_2), 3243(NH), 1692(C═O). ^{1}H NMR (400 MHz, $CDCl_3$) δ: 8.56 (dd, J = 7.3, 1.2 Hz, 2H, −ArH), 8.18 (dd, J = 8.3, 1.2 Hz, 2H, −ArH), 7.72 (dd, J = 8.2, 7.3 Hz, 2H, −ArH), 4.32 (t, J = 6.6 Hz, 2H, $-CH_2$), 2.99 (t, J = 6.6 Hz, 2H, $-CH_2$), 2.77−2.72 (m, J = 3.3 Hz, 4H, $-CH_2$). ^{13}C NMR (100 MHz, D_2O) δ: 165.54, 135.67, 131.80, 130.98, 127.10, 126.99, 120.27, 46.76, 44.54, 36.64, 35.29. HR-MS, m/z: $[M+H]^+$ 284.1401 (calcd for $C_{14}H_{12}N_2O_2^+$: 284.1392).

2.2.2. Synthesis of ferrocene appended mono-naphthalimide derivative **2**

Ferrocenecarboxaldehyde (0.53 g, 2.46 mmol) and compound **1** were dissolved in 50 mL methanol. After refluxed for 3 h, the mixture was cooled to room temperature. Then sodium borohydride (0.2 g, 4.92 mmol) was added in batches with constant stirring at room temperature. After the mixture was refluxed for 2 h, the solvent was removed by rotary evaporator to obtain the crude product. Then the crude product was dissolved in 50 mL dichloromethane, washed by 50 mL saturated sodium bicarbonate for two times, 50 mL water and 50 mL saturated brine in turn. The organic layer was dried by sodium sulfate. After the organic solvent was removed by rotary evaporator, pure product was obtained by column chromatography (ethyl acetate: methanol).

2.2.2.1. Ferrocene appended mono-naphthalimide derivative ***2a***. Yield: 56.48%. FTIR (KBr) ν: 3316(NH), 1698(C═O), 491(Cp-Fe-Cp). ^{1}H NMR (400 MHz, DMSO-d_6) δ: 8.49 (ddd, J = 16.6, 7.8, 1.1 Hz, 4H, −ArH), 7.88 (dd, J = 8.2, 7.3 Hz, 2H, −ArH), 4.25−4.17 (m, 4H, $-C_5H_4$), 4.11 (s, 5H, $-C_5H_5$), 4.07 (t, J = 1.9 Hz, 2H, $-CH_2$), 3.57 (s, 2H, $-CH_2$), 3.34 (s, 2H, $-CH_2$), 2.91 (t, J = 6.4 Hz, 2H, $-CH_2$). ^{13}C NMR (100 MHz, DMSO-d_6) δ: 163.59, 134.24, 131.26, 130.67, 127.39, 127.19, 122.14, 68.17, 67.18, 47.60, 46.25. HR-MS, m/z: $[M+H]^+$ 439.1082 (calcd for $C_{25}H_{23}FeN_2O_2^+$:439.1031).

2.2.2.2. Ferrocene appended mono-naphthalimide derivative ***2b***. Yield: 48.57%. FTIR (KBr) ν: 3369(NH), 1696(C═O), 495(Cp-Fe-Cp). ^{1}H NMR (400 MHz, DMSO-d_6) δ: 8.49 (ddd, J = 8.4, 5.1, 1.2 Hz, 4H, −ArH), 7.89 (dd, J = 8.3, 7.3 Hz, 2H, −ArH), 4.35 (t, J = 1.9 Hz, 2H, $-CH_2$), 4.23−4.14 (m, 8H, -FcH), 3.79 (s, 2H, $-CH_2$), 2.97−2.78 (m, 6H, $-CH_2$). ^{13}C NMR (100 MHz, DMSO-d_6) δ: 163.54, 134.23, 131.29, 130.67, 127.42, 127.18, 122.14, 68.15, 67.18, 47.84, 46.68, 46.37. HR-MS, m/z: $[M+H]^+$ 482.1529 (calcd for $C_{27}H_{28}FeN_3O_2^+$:482.1453).

2.2.3. Synthesis of *N*-(tert-butyloxyoxycarbonyl)-bis(2-hydroxyethyl)aminoethylamine **3**

To a solution of *N*-Boc-bromoethylamine (10 g, 44.62 mmol) and *N*-hydroxyethylenediamine (2.85 mL, 29.75 mmol) in 100 mL acetonitrile, anhydrous potassium carbonate (20.56 g, 150 mmol)

was added. The mixture was refluxed for 40 h. After filtrated to remove the solid, the filtrate was concentrated by rotary evaporator to obtain the crude product. The pure oil product was purified by column chromatography (ethyl acetate: methanol = 20:1, v/v). The yield of compound 3 was 20%. FTIR (KBr) ν: 3346(br, NH, OH), 1691(C═O). ^{1}H NMR (400 MHz, $CDCl_3$) δ: 3.90–3.74 (m, 4H, $-CH_2$), 3.44 (q, J = 5.5 Hz, 2H, $-CH_2$), 3.25–2.95 (m, 6H, $-CH_2$), 1.44 (d, J = 4.1 Hz, 9H, $-OC(CH_3)_3$). ^{13}C NMR (100 MHz, $CDCl_3$) δ: 159.51, 79.95, 62.31, 60.64, 55.69, 38.17, 28.51. HR-MS, m/z: $[M+H]^+$ 249.1802 (calcd for $C_{11}H_{25}N_2O_4^+$:249.1736).

2.2.4. Synthesis of bis-naphthalimide derivative **4**

1,8-Naphthalimide (2.67 g, 13.55 mmol), compound **3** (1.53 g, 6.16 mmol) and triphenylphosphine (4.8 g, 18.48 mmol) were dissolved in 50 mL anhydrous THF. After cooled to 0 °C in an ice-water bath, diisopropyl azodiformate (3.7 mL, 18.48 mmol) was added dropwise with stirring in 30 min. Then the mixture was stirred under the protection of nitrogen at room temperature for 5 h. After removed the solvent by rotary evaporator, the crude oil product was purified by column chromatography (ethyl acetate: petroleum ether = 1:1, v/v) to yield the pure product. The yield of compound **4** was 52.94%. FTIR (KBr) ν: 3349(NH), 1701(C═O). ^{1}H NMR (400 MHz, $CDCl_3$) δ: 8.51 (dd, J = 7.3, 1.1 Hz, 4H, −ArH), 8.24 (dd, J = 8.3, 1.1 Hz, 4H, −ArH), 7.73 (dd, J = 8.3, 7.3 Hz, 4H, −ArH), 4.74 (q, J = 7.6 Hz, 4H, $-CH_2$), 3.77 (s, 6H, $-CH_2$), 3.59 (s, 2H, $-CH_2$), 1.32 (s, 9H, $-OC(CH_3)_3$). ^{13}C NMR (100 MHz, DMSO-d_6) δ: 164.08, 163.82, 134.32, 131.25, 130.70, 127.47, 127.12, 122.01, 78.45, 28.02. HR-MS, m/z: $[M+H]^+$ 607.2551 (calcd for $C_{35}H_{35}N_4O_6^+$: 607.2558).

2.2.5. Synthesis of reference compound **5**

To a solution of Compound **4** (1.5 g, 2.47 mmol) in 30 mL dichloromethane, 15 mL trifluoroacetic acid (TFA) was added. After stirred for 2 h, 80 mL saturated sodium bicarbonate solution was slowly added. Then the water solution was extracted by 100 mL dichloromethane for 3 times. The organic layer was combined and dried by sodium sulfate. Dichloromethane was removed by rotary evaporator to obtain the pure product. The yield of compound 5 was 89.6%. FTIR (KBr) ν: 3177(NH_2), 1694(C═O). ^{1}H NMR (400 MHz, DMSO-d_6) δ: 8.43 (dd, J = 8.3, 1.1 Hz, 4H, −ArH), 8.30 (dd, J = 7.3, 1.2 Hz, 4H, −ArH), 7.81 (t, J = 7.8 Hz, 4H, −ArH), 4.12 (t, J = 6.8 Hz, 4H, $-CH_2$), 2.81 (t, J = 6.8 Hz, 4H, $-CH_2$), 2.61 (t, J = 6.5 Hz, 2H, $-CH_2$), 2.53 (d, J = 6.1 Hz, 2H, $-CH_2$). ^{13}C NMR (100 MHz, DMSO-d_6) δ: 163.42, 134.22, 131.22, 130.54, 127.32, 127.09, 121.97, 53.62, 51.59, 38.21, 37.64. HR-MS, m/z: $[M+H]^+$ 507.2028 (calcd for $C_{30}H_{27}N_4O_4^+$:507.1954).

2.2.6. Synthesis of ferrocene appended bis-naphthalimide derivative **6**

Ferrocenecarboxaldehyde (0.42 g, 1.96 mmol) and compound **5** (1.00 g, 1.97 mmol) were dissolved in 50 mL methanol. After refluxed for 3 h, the mixture was cooled to room temperature. Then sodium borohydride (0.15 g, 4.0 mmol) was added in batches with constant stirring at room temperature. After the mixture was refluxed for 2 h, the solvent was removed by rotary evaporator to obtain the crude product. The crude product was dissolved in 50 mL dichloromethane, washed by 50 mL saturated sodium bicarbonate for two times, 50 mL water and 50 mL saturated brine in turn. The organic layer was dried by sodium sulfate. After the organic solvent was removed by rotary evaporator, pure product was obtained by column chromatography (ethyl acetate: methanol = 3:1, v/v). The yield of compound **6** was 43.06%. FTIR (KBr) ν: 3349(NH), 1698(C═O), 485(Cp-Fe-Cp). ^{1}H NMR (400 MHz, DMSO-d_6) δ: 8.46 (d, J = 8.2 Hz, 4H, −ArH), 8.33 (d, J = 7.2 Hz, 4H, −ArH), 7.84 (t, J = 7.8 Hz, 4H, −ArH), 4.17–4.14 (m, 4H, $-C_5H_4$), 4.01 (s, 5H, $-C_5H_5$), 3.93 (t, J = 1.8 Hz, 2H, $-CH_2$), 3.88 (t, J = 1.9 Hz, 2H, $-CH_2$), 3.08 (s, 2H, $-CH_2$), 2.83 (t, J = 6.8 Hz, 4H, $-CH_2$), 2.67 (t, J = 6.2 Hz, 2H, $-CH_2$). ^{13}C NMR (100 MHz, DMSO-d_6) δ: 163.39, 134.17, 131.24, 130.54, 127.34, 127.08, 122.00, 68.31, 68.18, 67.32, 51.62, 37.61. HR-MS, m/z: $[M+H]^+$ 705.2162 (calcd for $C_{41}H_{37}FeN_4O_4^+$:705.2086).

2.3. Water solubility

Excess amount (more than 10 mg for each compound) naphthalimide compounds were added into 5 mL volumetric flask, respectively. After the addition of distilled water, the mixture was ultrasonic treatment for 30 min until the compounds were dissolved adequately in water to form a saturation solution. Then the saturation solution was stored in dark for 24 h. The supernatant was moved to centrifuge tubes and centrifuged for 15 min, then filtrated by microfiltration membrane to obtain the test solution. After dilution, the absorbance of the test solution was measured by UV–Vis spectrophotometer. And the saturation solubility of the compounds was calculated according to the standard curve of each compound.

2.4. Electrochemical studies

A three electrode system was used to study the electrochemical properties of the ferrocene appended naphthalimide compounds. The working electrode, auxiliary electrode and reference electrode were glassy carbon electrode, platinum electrode and Ag/AgCl/KCl (sat.), respectively. The tested compounds were dissolved in 50% DMSO water solution as storage solution (10 mmol/L). Then 1 mL compound solution was diluted to 10 mL by 90% ethanol solution containing tetra-*n*-butylammonium perchlorate (TBAP, 0.1 mol/L) as the supporting electrolyte. The scan rate was 100 mV/s in the experiment.

2.5. Ethidium bromide displacement experiment

200 μL stock solution of EB (1 mg/mL) was added into a 50 mL volumetric flask. Then diluted with PBS buffer solution (10 mmol/L, pH 7.4) to volume. To another 163 μL stock solution of CT DNA (1 mg/mL) in 25 mL volumetric flask was diluted by the prepared EB-PBS buffer solution to volume. The maximum fluorescence intensity of the EB-DNA PBS buffer solution was measured on a Hitachi F4600 spectrofluorometer at room temperature as F_0. In 3 mL EB-DNA PBS buffer solution, increasing volume of the compounds solution (5 mmol/L in DMSO, 5–15 μL) were added. And the maximum fluorescence intensity of the mixture solution was measured as F. The quenching constants were calculated according to the Stern-Volmer equation [15].

$$F_0/F = 1 + K_{sv}[\text{Compound}]$$

Where K_{sv} is the quenching constant.

2.6. UV–visible spectrophotometry

20 μL stock solution of naphthalimide compounds (5 mmol/L in DMSO) was diluted by 3 mL phosphate buffer (10 mmol/L, pH = 7.4). Increasing volume of CT DNA solution (10–30 μL, 1 mg/mL) was added into the solution. The UV–Vis spectra of the compounds were recorded by a Shimadzu UV-2600 spectrophotometer. And the molar absorption coefficient of the compounds at 341 nm was calculated according to the recorded data as ε_f. Then the solution was stirred and incubated at room temperature for 10 min. After that, the UV–Vis spectra in the absence and presence of DNA were recorded by a Shimadzu UV-2600 spectrophotometer. The binding constant K_a was calculated from a $D/\Delta\varepsilon_{ap}$ vs D plot

according to the following equation [16].

$$D/\Delta\varepsilon_{ap} = D/\Delta\varepsilon + 1/[(\Delta\varepsilon)K_a]$$

Where D is the concentration of DNA, $\Delta\varepsilon_{ap} = [\varepsilon_a\text{-}\varepsilon_f]$, $\varepsilon_a = A_{obs}/$[compound], $\Delta\varepsilon = [\varepsilon_b\text{-}\varepsilon_f]$, ε_b and ε_f correspond to the extinction coefficients of the DNA-compound adduct and unbound compound, respectively.

2.7. Viscosity studies

Naphthalimide compounds were dissolved in 30% DMSO/water solution as storage solution (5 mmol/L). 0.5 mL CT DNA (1 mg/mL) was diluted by 20 mL phosphate buffer (10 mmol/L, pH 7.4) in an Ubblehode viscometer. After the mixture was equilibrated in a water bath at 25 °C for 10 min, the flow time was measured by stopwatch after varying the concentrations of compounds. The plot of $(\eta/\eta_0)^{1/3}$ vs r was obtained according to the flow time, where η and η_0 were the flow time of presence and absence of compounds, respectively, and r was equal to [compound]/[DNA].

2.8. Cytotoxicity assay

Human esophageal carcinoma cell (EC109), Human gastric carcinoma cell line (BGC823), human gastric cancer (SGC7901) were cultured in RPMI 1640 medium, and hepatoblastoma cell line (HepG2) were cultured in DMEM medium supplemented with 10% fetal bovine serum, 10 units/mL penicillin, and 10 units/mL penicillin streptomycin. Cell culture was kept in 5% CO_2 under humidified conditions at 37 °C. The culture solution was changed every other day, and the subcultures were performed with 0.25% trypsin. Tested compounds were solubilized in RPMI 1640 or DMEM medium and diluted to different concentration right after it will be used.

The thiazolyl blue tetrazolium bromide (MTT) assay was used to evaluate the cytotoxicity of synthesized naphthalimide in vitro. Tumor cells were planted into 96-well microtiter plates at a density of 5.0×10^3 cells/well. After cultured in 5% CO_2 under humidified conditions at 37 °C for 24 h, various compounds medium solution were added to obtain the final drug concentration of 0, 6.25, 12.5, 25, 50 and 100 μmol/L, respectively. 50 μL MTT (5 mg/L) was added into each cell after 24 h incubation. For 4 h later, the medium was removed and replaced by 150 μL DMSO to solubilize the converted purple dye in culture plates. The absorbance of each cell was measured by a Bio-rad 680 microplate reader at 550 nm. The IC_{50} which inhibits the growth of 50% of cells relative to nontreated control cells was calculated as the concentration of tested compound by linear fitting.

2.9. Cellular uptake and localization

After HepG2 cells were seeded into well plates 2×10^5 cells/well for 24 h, compound **6** (6 μmol/L) was added into the well plates. After incubation for 12 h, the culture supernatant was removed and the cells were washed by PBS buffer for 3 times. Then paraformaldehyde solution was added and incubated with cells for 15 min to fix the cells. After that, the cells were washed by PBS buffer again, then stained with DAPI. The images were captured using an Olympus FV1000-IX81 Confocal Microscope.

2.10. Comet assay

HepG2 cells were planted into 6-well microtiter plates. After cultured in 5% CO_2 under humidified conditions at 37 °C for 24 h, compound 6 was added to obtain the final drug concentration of 7, 11 and 15 μmol/L, respectively. 0.5% DMSO was used as control group. After incubation for 24 h, cells were washed by PBS buffer for comet test experiment.110 μL 0.8% normal melting point agarose was precoated on a microscope slide. Then 100 μL 0.8% low melting point agarose with 10^4 cells was frosted on the precoated microscope slide at 4 °C. After that, the slide was immersed in a lysis solution (2.5 mol/L NaCl, 100 mmol/L Na_2EDTA, 10 mmol/L Tris, 1% Sodium Sarcosinate, 1% TritonX-100, pH 10.0) for 3 h. After the lysis immersion, the slide was placed in a horizontal electrophoresis tank containing an electrophoretic solution (1 mmol/L NaEDTA, 300 mmol/L NaOH, pH 13.0) for 30 min. Then electrophoresis was carried out at 22 V, 190 mA condition for 40 min. After electrophoresis, the slide was washed by PBS buffer for 3 times and stained with EB. Comets were visualized with an Olympus BX53 fluorescence microscopy. 100 cells were randomly selected for recording the tail DNA% and tail moment.

2.11. Statistical analysis

The significance of the differences between values obtained through comet assay was evaluated using one-way ANOVA, followed by LSD *t*-test, statistically different from the control: $^{**}p < 0.01$.

3. Results and discussion

3.1. Chemistry

The synthesis route of ferrocene appended naphthalimide derivatives was shown in Scheme 1. In the synthesis of mono-naphthalimide derivatives, firstly, 1,8-naphthalimide was reacted with the hydroxyl group of different amino alcohols via Mitsunobu Reaction. And the amino terminus of the amino alcohols was condensed with ferrocenecarboxaldehyde by Schiff's base reaction. Then the different Schiff bases were reduced by sodium borohydride to yield the target compound **2**. In the synthesis of bis-naphthalimide derivative 6, due to the steric hindrance of the naphthalimide group, the alkylation reaction of *N*-Boc-bromoethylamine with di(naphthalimidoethyl) amine **7** failed. Hence, a modified synthesis route of compound **6** was started from the alkylation reaction of *N*-Boc-bromoethylamine with diethanolamine. Then the intermediate **3** was condensed with 1,8-naphthalimide via Mitsunobu Reaction to obtain compound **4**. After compound **4** was deprotected by TFA to yield the reference compound **5**, the amino group of compound **5** was condensed with ferrocenecarboxaldehyde and reduced by sodium borohydride to obtain the target compounds **6**. All of the synthesized compounds were characterized by IR, ^1H NMR, ^{13}C NMR and mass spectroscopies.

The IR spectral data of the ferrocene appended naphthalimide derivatives were shown in Table 1. The broad band at ~3350 cm^{-1} owed to the stretching of *N*—H and the sharp peak at ~1698 cm^{-1} was due to the stretching of C=O. And the characteristic peak of the ferrocene group was observed at ~490 cm^{-1} [17]. In the ^1H NMR spectra of ferrocene appended naphthalimide derivatives, the characteristic peaks of naphthalimide and ferrocene group were displayed around 7.84—8.49 ppm and 4.01—4.25 ppm, respectively.

3.2. Electrochemical studies

The electrochemical property of the synthesized ferrocene appended naphthalimide derivatives was studied by cyclic voltammetry (CV) in 90% ethanol water solution. All prepared ferrocene appended naphthalimide derivatives exhibited reversible one-electron redox process (Fig. 2), which was due to the

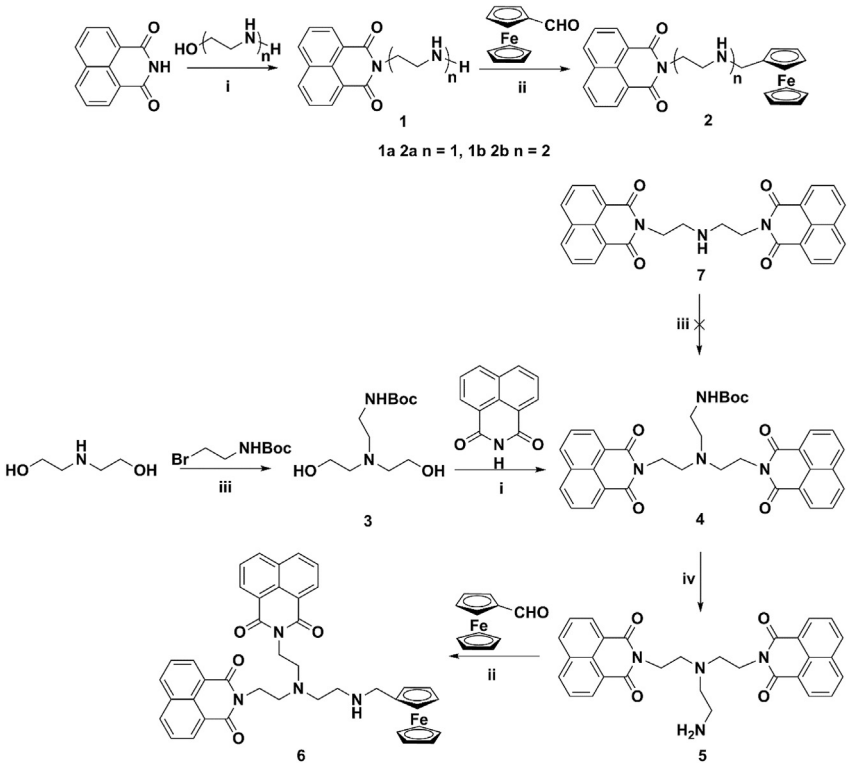

Scheme 1. Synthesis route of ferrocene appended naphthalimide derivatives. i) PPh_3, DIAD, ii) $NaBH_4$, iii) K_2CO_3, iv) TFA.

Table 1
IR (ν in cm^{-1}) spectroscopic data of ferrocene appended naphthalimide derivatives (2a, 2b and 6).

Compounds	ν_{NH}	$\nu_{C=O}$	$\nu_{Cp\text{-}Fe\text{-}Cp}$
2a	3316	1698	491
2b	3369	1696	495
6	3349	1698	485

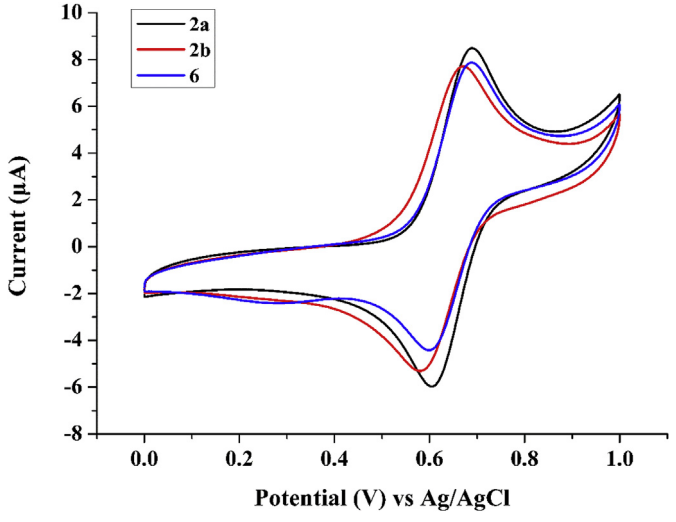

Fig. 2. The CV curves of ferrocene appended naphthalimide derivatives. (0.1 mmol/L in 90% ethanol water solution, 0.1 mol/L TBAP, scan rate 100 mV/s).

formation of ferrocene/ferrocenium redox couple [18]. The oxidation peaks of compound **2a**, **2b** and **6** were at 690 mV, 672 mV and 689 mV, respectively. And the reduction peaks were at 604 mV, 580 mV and 599 mV, respectively. The ΔE values for the studied compounds were more than 59 mV, which was attributed to the uncompensated solution resistance [19].

3.3. Ethidium bromide displacement experiment

EB is a typical DNA intercalator with strong fluorescence intensity when binding with DNA duplexes. After the addition of other DNA intercalator into EB-DNA complex solution, EB molecules which inserting into the DNA base pairs are replaced by the intercalator and the fluorescence intensity of the EB-DNA complex solution is quenched [20]. The fluorescence quenching constants are calculated by Stern-Volmer equation and used to evaluate the DNA binding mode and binding ability of the intercalators [9c,21]. In our experiments, the fluorescence intensity of the EB-DNA complex solution was decreased in the addition of synthesized naphthalimide derivatives (Fig. 3). And the fluorescence quenching constants were 1.53×10^5 L/mol, 1.70×10^5 L/mol, 2.04×10^5 L/mol and 3.37×10^5 L/mol for compounds **2a**, **2b**, **5** and **6**, respectively. It was no doubt that the fluorescence quenching constants of bis-naphthalimide compounds were larger than the mono-naphthalimide compounds. To our surprise, the quenching constants of bis-naphthalimide hybrid compound **6** were 1.65 times larger than that of the reference compound **5**. The enhanced quenching constants of ferrocene appended bis-naphthalimide derivative **6** might be due to the groove binding of ferrocene group [22]. According to the calculated quenching constants, intercalation might be the binding mode for all of the compounds.

3.4. UV–visible spectrophotometry

The EB displacement experiment is an indirect way to study the interaction of small molecules with DNA. UV–Vis absorption study is another important technique to evaluate the DNA binding ability

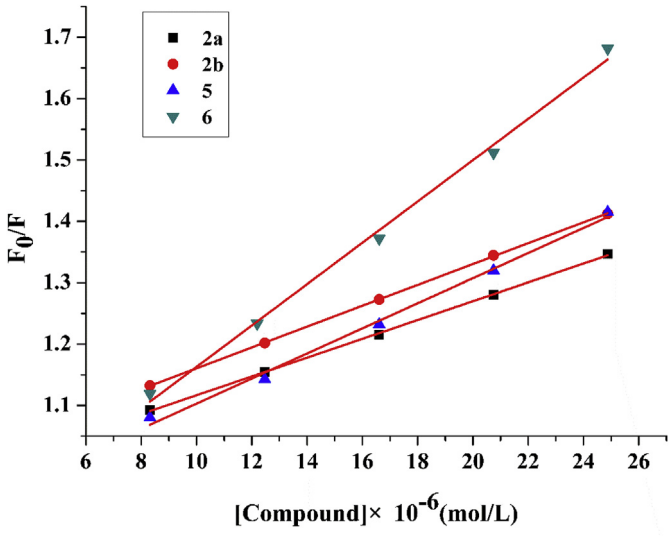

Fig. 3. Stern-Volmer plot of the EB displacement experiments of naphthalimide derivatives 2, 5 and 6. [DNA] = 20 μmol/L, [EB] = 10 μmol/L.

of small molecules [9c,23]. In an effort to further understand the role of the ferrocene group in hybrid compound **6**, UV−visible spectrophotometry was carried out to evaluate the interaction of reference compound **5** and **6** with DNA. As shown in Fig. 4, the maximum absorption wavelength of the compounds was at 341 nm, which was attributed to the absorption of the naphthalimide group. The UV−Vis spectra of both compounds were showed a significant hypochromic effect after the addition of DNA, which indicated the intercalation binding mode between the compounds with DNA duplex [21]. According to the data, the binding constant of compound **5** and **6** were calculated as 1.22×10^4 L/mol and 1.35×10^4 L/mol, respectively. Ferrocene appended bis-naphthalimide derivative **6** was exhibited higher binding constant than the reference compound **5**, which was in accordance with the results of EB displacement experiments. That is to say, the conjugation of ferrocene in the amino terminus is helpful to improve the DNA binding ability of naphthalimide derivative.

3.5. Viscosity studies

Viscosity studies is a useful method to evaluate the binding mode of small molecules with DNA. In typical intercalation binding mode, the aromatic ring intercalate between the base pairs of DNA duplex and prolong the length of DNA, which increase the viscosity of DNA solution. The viscosity results of the naphthalimide derivatives were shown in Fig. 5. The classic DNA intercalator EB was used as reference compound. Compared with EB, all the naphthalimide derivatives did not show the typical intercalation binding mode with DNA. The viscosity of DNA solution was slightly increased then dropped after the addition of mono-naphthalimide derivatives. The appended ferrocene group disturbed the typical intercalation binding mode of naphthalimide [24]. And the addition of bis-naphthalimide derivatives induced a dramatic decline of the viscosity of DNA solution, which meant the partial intercalation of naphthalimide groups [25].

3.6. In vitro cytotoxicity

The cytotoxicity of ferrocene appended naphthalimide derivatives and reference compound **5** against **4** different cancer cell

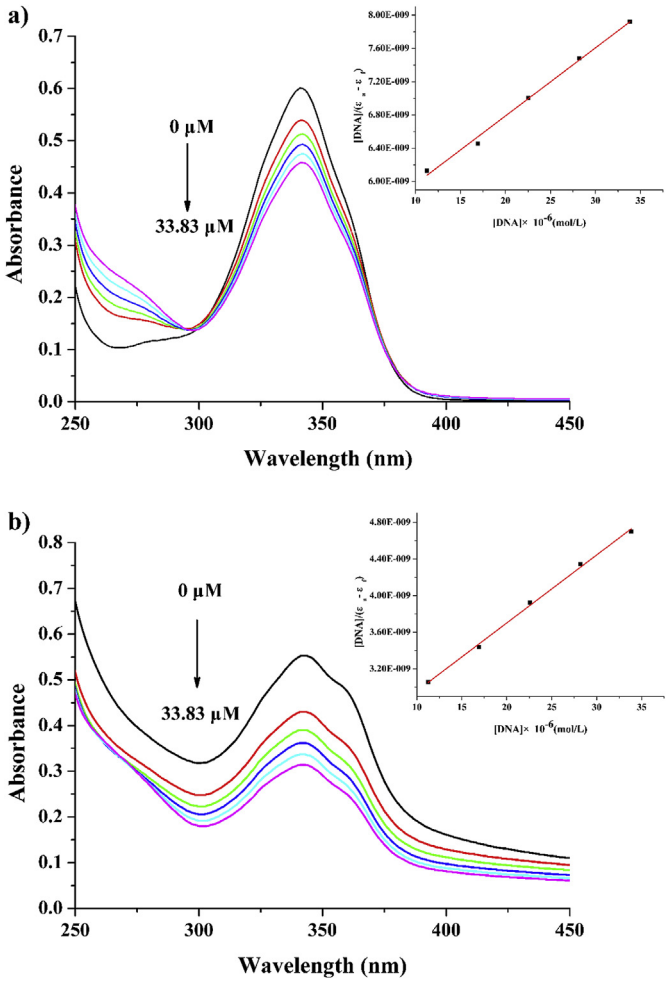

Fig. 4. UV−Vis spectra of naphthalimide derivatives 5 (a) and 6 (b) in phosphate buffer (10 mmol/L, pH = 7.4). Inset: Plots of [DNA]/(εa-εf) vs. [DNA].

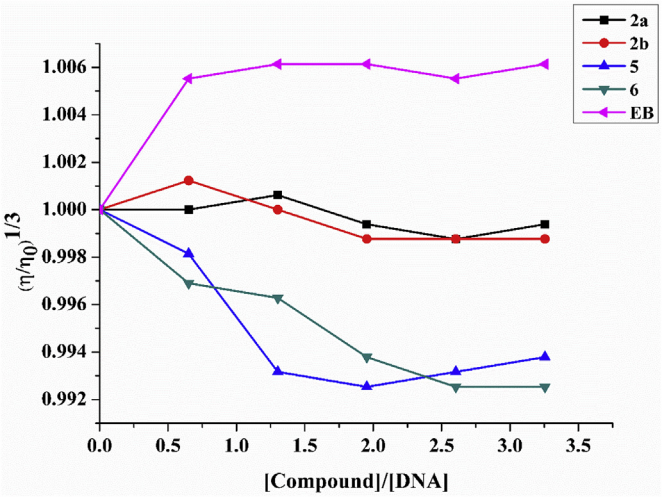

Fig. 5. DNA viscosity titration of naphthalimide derivatives at 25 °C in phosphate buffer (10.0 mM, pH 7.4).

lines EC109, BGC823, SGC 7901 and HepG2 were evaluated by MTT colorimetric assay (Table 2). Although the tendency of the cytotoxicity was in accordance with that of the binding ability, the

Table 2
The cytotoxicity of naphthalimide derivatives.

Compounds	Cytotoxicity (IC_{50} μmol/L)			
	EC109	BGC823	SGC 7901	HepG2
2a	>200	>200	>200	>200
2b	113.70	88.16	68.54	123.90
5	67.86	62.84	31.00	120.00
6	10.52	7.76	4.33	6.79
Amonafide	129.00	80.14	52.17	34.64

binding ability was not the only factor which influenced the anticancer activity. According to the results of mono-naphthalimide derivatives, the cytotoxicity of ferrocene appended naphthalimide derivative **2a** and **2b** was lower than that of the control drug amonafide, which might be due to the lack of protonated amino substituent group [26] and the low solubility in the cell culture medium [27]. The water solubility of **2a** and **2b** was 1.60×10^{-4} and 1.53×10^{-3} mol/L, respectively (Table S1). The water solubility of **2b** was 10 times than that of **2a**. Comparing with the ethylene amine linker of **2a**, the extended diethylene amine linker of **2b** improved the hydrophilicity. The amount of the amine motif rather than the length of the linker improved the potency of naphthalimide [28]. For bis-naphthalimide derivatives, although the dimeric naphthalimide derivatives attracted attention, the success of this strategy depended on suitable linkers between two naphthalimide groups [29]. With the help of flexible polyamine linker, the bis-naphthalimide compounds **5** and **6** displayed higher cytotoxicity than the mono-naphthalimide ones. Importantly, the ferrocene appended bis-naphthalimide derivative **6** was the most active compound in all of the tested naphthalimide derivatives against cancer cell lines. The IC_{50} values of compound **6** were found to be 10.52 μmol/L, 7.76 μmol/L, 4.33 μmol/L and 6.79 μmol/L on EC109, BGC823, SGC 7901 and HepG2 cells, respectively, which were much better than the control drug amonafide and the reference compound **5**. Considering the ability of ferrocene in promoting the generation of free radicals [5b], the synergistic effect between ferrocene group and bis-naphthalimide derivative significantly enhanced the cytotoxicity [30].

3.7. Cellular uptake and localization

Due to the strong green fluorescence and superior photostability, naphthalimide is widely used in fluorescence chemosensors [31] and fluorescent cellular imaging agents [10b]. Hence, the cellular uptake and localization of bis-naphthalimide derivative **6** were able to study by confocal microscopy. DAPI, a nucleus-specific blue fluorescence dye was used for co-localization study. As shown in Fig. 6, after 12 h incubation of HepG2 cells with compound **6**, the cells were stained by compound **6** and green fluorescence was observed (Fig. 6a). Blue fluorescence was observed for DAPI (Fig. 6b), which was located in the nucleus of the cells. The merged image (Fig. 6c) confirmed the uptake of bis-naphthalimide derivative **6** which was located in the cytosol and nucleus of the cancer cells.

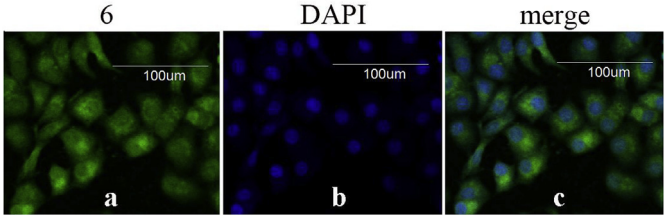

Fig. 6. Confocal microscopic images of HepG2 cells treat with bis-naphthalimide derivative 6 (a), DAPI (b) and merge (c).

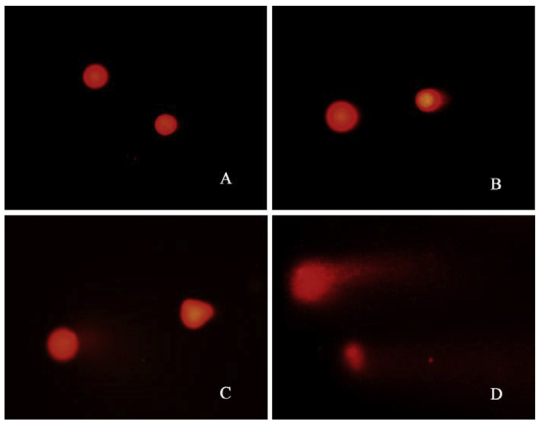

Fig. 7. Photomicrographs of DNA damage evaluated by comet assay for HepG2 treated with different concentration of bis-naphthalimide derivative 6. (A) Control group, 0 μmol/L (B) 7 μmol/L (C) 11 μmol/L (D) 15 μmol/L.

3.8. Comet assay

Comet assay is a useful technique to evaluate the rate of DNA damages at the level of individual cells [32]. As shown in Fig. 7, the undamaged cells exhibited comets with no tails. After treated with bis-naphthalimide derivative **6**, the cells showed comets with detectable tails. Comparing with the control group, the tail DNA (%) and tail moment ratio of treated cells increased with the increase of the concentration of bis-naphthalimide derivative **6** (Table 3). The tail DNA (%) and tail moment ratio of the cells in the control group were $2.07 \pm 0.36\%$ and 0.89 ± 0.34, respectively. After treated by bis-naphthalimide derivative **6**, the tail DNA (%) increased from $6.54 \pm 1.44\%$ to $14.96 \pm 4.86\%$ and the tail moment ratio increased from 2.26 ± 0.72 to 126.14 ± 24.58 by increasing the concentration from 7 μmol/L to 15 μmol/L. The DNA of HepG2 cells showed significant damage ($p < 0.01$) induced by bis-naphthalimide derivative **6** at 15 μmol/L. This results indicated that bis-naphthalimide derivative **6** was able to cause DNA damage in cancer cells.

4. Conclusions

Herein, some ferrocene appended naphthalimide derivatives were synthesized and characterized to evaluate the synergistic effect of the ferrocene group in anticancer activity of napthalimide derivatives. And according to the results of EB display, UV–visible spectrophotometry and viscosity studies, the ferrocene appended naphthalimide derivatives exhibited partial-intercalation binding mode with DNA duplex. Ferrocenyl group was helpful to enhance the DNA binding ability of bis-naphthalimide derivative. Hybrid compound **6** was 6.45–17.62 times more toxicity than the reference compound **5** and control drug amonafide on tested cancer cell lines.

Table 3
DNA damage induced by bis-naphthalimide derivative 6 in HepG2 cells.

	Control	7 μmol/L	11 μmol/L	15 μmol/L
Tail DNA (%)	2.07 ± 0.36	6.54 ± 1.44	8.29 ± 1.90	$14.96 \pm 4.86^{**}$
Tail Moment	0.89 ± 0.34	2.26 ± 0.72	8.64 ± 7.20	$126.14 \pm 24.58^{**}$

$^{**}p < 0.01$ in comparison to control group using ANOVA LSDt test.

The synergistic effect of ferrocene group played an important role to enhance the cytotoxicity of bis-naphthalimide derivative. And the cytotoxicity of compound **6** was relate to the DNA damage in cancer cells.

Acknowledgments

This work was financially supported by the National Natural Science Foundation of China (Nos. 21362026, 21867016), Young Talent Program of NingXia medical University and Ningxia Medical University Key Project (XZ2018002).

Appendix A. Supplementary data

Supplementary data to this article can be found online at https://doi.org/10.1016/j.jorganchem.2019.03.001.

References

[1] World Health Organization, Cancer. http://www.who.int/en/news-room/fact-sheets/detail/cancer. (Accessed 28 September 2018).
[2] Global Cancer Facts & Figures, third ed., American Cancer Society., 2015.
[3] L.M. Jarvis, Chem. Eng. News 96 (2018) 26–30.
[4] a) M. Hanif, C.G. Hartinger, Future Med. Chem. 10 (2018) 615–617;
b) M. Yang, U. Bierbach, Eur. J. Inorg. Chem. (2017) 1561–1572;
c) G. Gasser, I. Ott, N. Metzler-Nolte, J. Med. Chem. 54 (2011) 3–25.
[5] a) C. Ornelas, New J. Chem. 35 (2011) 1973–1985;
b) D. Astruc, Eur. J. Inorg. Chem. (2017) 6–29, a) C. Ornelas, New Journal Of Chemistry 2011, 35, 1973-1985; b) D. Astruc, European Journal Of Inorganic Chemistry 2017, 6-29.
[6] a) K. Kowalski, A. Koceva-Chyla, L. Szczupak, P. Hikisz, J. Bernasinska, A. Rajnisz, J. Solecka, B. Therrien, J. Organomet. Chem. 741 (2013) 153–161;
b) W.H. Mahmoud, N.F. Mahmoud, G.G. Mohamed, J. Organomet. Chem. 848 (2017) 288–301;
c) M. Mbaba, A.N. Mabhula, N. Boel, A.L. Edkins, M. Isaacs, H.C. Hoppe, S.D. Khanye, J. Inorg. Biochem. 172 (2017) 88–93;
d) A. Kondratskyi, K. Kondratska, F.V. Abeele, D. Gordienko, C. Dubois, R.A. Toillon, C. Slomianny, S. Lemiere, P. Delcourt, E. Dewailly, R. Skryma, C. Biot, N. Prevarskaya, Sci. Rep-UK 7 (2017) 15896;
e) P. Pigeon, Y. Wang, S. Top, F. Najlaoui, M.C.G. Alvarez, J. Bignon, M.J. McGlinchey, G. Jaouen, J. Med. Chem. 60 (2017) 8358–8368;
f) W.A. Wani, E. Jameel, U. Baig, S. Mumtazuddin, L.T. Hun, Eur. J. Med. Chem. 101 (2015) 534–551.
[7] a) ClinicalTrials.gov Identifier: NCT02497612. https://clinicaltrials.gov/ct2/show/record/NCT02497612. (Accessed 28 September 2018);
b) ClinicalTrials.gov Identifier: NCT03660839. https://clinicaltrials.gov/ct2/show/record/NCT03660839. (Accessed 28 September 2018).
[8] K. Kowalski, Coord. Chem. Rev. 366 (2018) 91–108.
[9] a) A.C. Matsheku, M.Y.H. Chen, S. Jordaan, S. Prince, G.S. Smith, B.C.E. Makhubela, Appl. Organomet. Chem. 31 (2017), e3852;
b) C.W. Ong, J.Y. Jeng, S.S. Juang, C.F. Chen, Bioorg. Med. Chem. Lett 2 (1992) 929–932;
c) R. Singh, P.R. Devi, S.S. Jana, R.V. Devkar, D. Chakraborty, J. Organomet. Chem. 849–850 (2017) 157–169.
[10] a) A. Kamal, N.R. Bolla, P.S. Srikanth, A.K. Srivastava, Expert Opin. Ther. Pat. 23 (2013) 299–317;
b) S. Banerjee, E.B. Veale, C.M. Phelan, S.A. Murphy, G.M. Tocci, L.J. Gillespie, D.O. Frimannsson, J.M. Kelly, T. Gunnlaugsson, Chem. Soc. Rev. 42 (2013) 1601–1618.
[11] G. Gellerman, Lett. Drug Des. Discov. 13 (2016) 47–63.
[12] a) R.X. Rong, Q. Sun, C.L. Ma, B. Chen, W.Y. Wang, Z.A. Wang, K.R. Wang, Z.R. Cao, X.L. Li, Med. Chem. Comm. 7 (2016) 679–685;
b) R.X. Rong, S.S. Wang, X. Liu, R.F. Li, K.R. Wang, Z.R. Cao, X.L. Li, Bioorg. Med. Chem. Lett 28 (2018) 742–747.
[13] a) Y. Huang, C.X. Wu, Y. Song, M. Huang, D.N. Tian, X.B. Yang, Y.R. Fan, Molecules 23 (2018) 266;
b) Y. Huang, Y. Song, M. Huang, Y.R. Fan, D.N. Tian, Q.P. Zhao, X.B. Yang, W.N. Zhang, Res. Chem. Intermed. 42 (2016) 7329–7344;
c) Y. Huang, J.L. Liu, J. Zhang, Q. Liu, J.T. Hou, Y. Zhang, D.W. Zhang, Q.S. Lu, S.Y. Chen, H.H. Lin, X.Q. Yu, Sci. China Chem. 53 (2010) 103–112;
d) Y. Huang, Y. Zhang, J. Zhang, D.W. Zhang, Q.S. Lu, J.L. Liu, S.Y. Chen, H.H. Lin, X.Q. Yu, Org. Biomol. Chem. 7 (2009) 2278–2285.
[14] D. Yuan, X.W. Du, J.F. Shi, N. Zhou, A.A. Baoum, B. Xu, Beilstein J. Org. Chem. 10 (2014) 2406–2413.
[15] J.R. Lakowicz, G. Weber, Biochemistry 12 (1973) 4161–4170.
[16] C.V. Kumar, E.H. Asuncion, J. Am. Chem. Soc. 115 (1993) 8547–8553.
[17] V. Kudar, V. Zsoldos-Mady, K. Simon, A. Csampai, P. Sohar, J. Organomet. Chem. 690 (2005) 4018–4026.
[18] I. Noviandri, K.N. Brown, D.S. Fleming, P.T. Gulyas, P.A. Lay, A.F. Masters, L. Phillips, J. Phys. Chem. B 103 (1999) 6713–6722.
[19] I.V. Smolyaninov, A.I. Poddel'sky, S.V. Baryshnikova, V.V. Kuzmin, E.O. Korchagina, M.V. Arsenyev, S.A. Smolyaninova, N.T. Berberova, Appl. Organomet. Chem. 32 (2018) e4121.
[20] R.F. Pasternack, M. Caccam, B. Keogh, T.A. Stephenson, A.P. Williams, E.J. Gibbs, J. Am. Chem. Soc. 113 (1991) 6835–6840.
[21] Y.Y. Zhou, T. Song, Y. Cao, G.D. Gong, Y.J. Zhang, H.H. Zhao, G. Zhao, J. Organomet. Chem. 871 (2018) 1–9.
[22] Y.T. Ding, Q.X. Wang, F. Gao, F. Gao, Electrochim. Acta 106 (2013) 35–42.
[23] A.A. Altaf, N. Khan, B. Lal, A. Badshah, J. Coord. Chem. 70 (2017) 3523–3540.
[24] A.B. Wu, Y.F. Xu, X.H. Qian, Bioorg. Med. Chem. 17 (2009) 592–599.
[25] S. Satyanarayana, J.C. Dabrowiak, J.B. Chaires, Biochemistry 32 (1993) 2573–2584.
[26] L.J. Xie, Y.F. Xu, F. Wang, J.W. Liu, X.H. Qian, J.N. Cui, Bioorg. Med. Chem. 17 (2009) 804–810.
[27] I. Ott, Y.F. Xu, X.H. Qian, J. Photochem. Photobiol., B 105 (2011) 75–80.
[28] Z.Y. Tian, S.Q. Xie, Y.W. Du, Y.F. Ma, J. Zhao, W.Y. Gao, C.J. Wang, Eur. J. Med. Chem. 44 (2009) 393–399.
[29] a) P. Yang, Q. Yang, X.H. Qian, Tetrahedron 61 (2005) 11895–11901;
b) G.A. Barron, G. Bermano, A. Gordon, P.K.T. Lin, Eur. J. Med. Chem. 45 (2010) 1430–1437;
c) R. Filosa, A. Peduto, S. Di Micco, P. de Caprariis, M. Festa, A. Petrella, G. Capranico, G. Bifulco, Bioorg. Med. Chem. 17 (2009) 13–24.
[30] M.D. Tomczyk, K.Z. Walczak, Eur. J. Med. Chem. 159 (2018) 393–422.
[31] R.M. Duke, E.B. Veale, F.M. Pfeffer, P.E. Kruger, T. Gunnlaugsson, Chem. Soc. Rev. 39 (2010) 3936–3953.
[32] a) N.P. Singh, M.T. McCoy, R.R. Tice, E.L. Schneider, Exp. Cell Res. 175 (1988) 184–191;
b) P.L. Olive, J.P. Banath, Nat. Protoc. 1 (2006) 23–29.